

Progress and Perspectives on strategies to control photochemical properties in Metallo-Dithiolene Donor-Acceptor systems.

This mini-review is dedicated to Prof. Renato Ugo, in memory of his seminal contribution to Chemistry and its applications in advances fields, including second-order nonlinear optics

Authors: Flavia Artizzu,^{a,*} Davide Espa,^b Luciano Marchiò,^c Luca Pilia,^{b,*} Angela Serpe^d and Paola Deplano^{d,*}

^a Dipartimento di Scienze e Innovazione Tecnologica, Università del Piemonte Orientale, viale Teresa Michel 11, 15121 Alessandria (Italy)

^b Dipartimento di Ingegneria Meccanica, Chimica e dei Materiali, Università di Cagliari, Via Marengo 2, 09123 Cagliari (Italy).

^c Dipartimento SCVSA, Università di Parma, Parco Area delle Scienze 17/a, 43124, Parma (Italy).

^d Dipartimento di Ingegneria Civile, Ambientale e Architettura, INSTM Research Unit, Università di Cagliari, Via Marengo 2, 09123 Cagliari (Italy)

flavia.artizzu@uniupo.it; pilialuc@unica.it; deplano@unica.it

Abstract. In this mini-review recent progress in studies on heteroleptic d^8 -metal dithiolenes complexes with a D–M–A donor– π –acceptor electronic structure showing non-linear and linear optical properties are presented. The ligands, formally dithiolenes, consist in a variety of donors (dithiolato) and acceptors (dithioamide and dithioamidate), differing for electronic properties and/or structural features, varying from rigid and planar systems to conformationally-flexible ones. It is shown how the components of these D–M–A systems modulate both the energy and topology of the frontier molecular orbitals involved in the charge transport mechanism to reach a fine tuning of the optical properties and achieve high values of the quadratic hyperpolarizability. Further tailoring of the ligands by integrating specific functional groups in their periphery, such as NH and/or a quinoxaline ring, is presented as a versatile tool to achieve a reversible response to external stimuli. Accordingly, selected cases where exchange color proton and silver ions tunable properties, switching of the NLO-response (with a 2.5 - 6.5 contrast for HCl exchange) and also uncommon emission color reversibly tuneable by different stimuli, such as proton and silver ions, are presented. In the bulk, crystals gave a poor or null SHG response, while a stable and large response has been obtained in a limited number of cases of complexes dispersed in PMMA films. Reported results are addressed to stimulate further work to exploit the potential of this class of complexes as molecular sensors and switches and to optimize the processing procedures to achieve good SHG responses in the bulk.

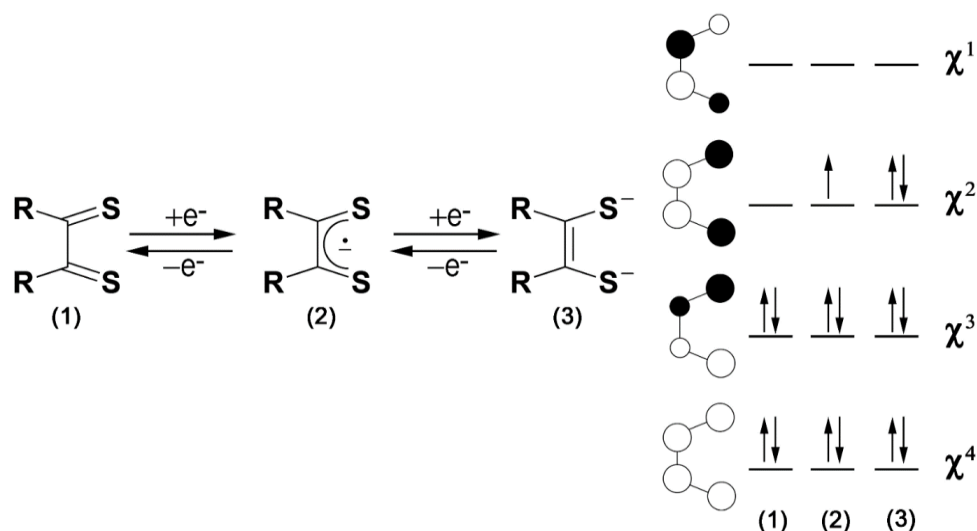
Keywords: Donor Acceptor Systems; d^8 -metals; Dithiolenes; Quadratic Hyperpolarizability; Fluorescence; Optical Switches

Introduction

Donor–acceptor conjugated molecules (D- π -A) represent a versatile class of compounds that, due to their inherent low-energy intramolecular charge-transfer (ICT) band in the visible to the near infrared (NIR) region, are of interest as building blocks for advanced photonic materials. In particular they can work as second-order nonlinear (NLO) chromophores. Second-order NLO effects arise from the first hyperpolarizability β , which at the molecular level relates to the way in which the mobile electronic charges respond to the oscillating electric field of a laser beam [1]. To observe quadratic NLO effects in the bulk, a polar ordering of the NLO chromophore, resulting in second harmonic generation (SHG), is required and different strategies can be employed to achieve this goal [2]. A versatile one comprises the formation of poled polymers, where the required asymmetry is imposed by the external electric field, while heating [3]. Among other strategies, the introduction of chiral groups in the molecules represents a chance to obtain crystals in a suitable non-centrosymmetric space group [4].

Several organic D- π -A molecules have been and still are extensively investigated as 2nd NLO-phores [5-10]. In addition suitable transition metal complexes, where the metal works as a π -bridge between the Donor and Acceptor ligands, play an important role in this field because they can provide improved stability for ligands and suitable-metals can favor co-planarity through their preferred coordination geometry, maximizing the CT Donor-Acceptor transition [11]. Moreover the opportunity to properly engineer the organic ligands, can favor the incorporation of the metal-complexes into suitable polymeric matrices and allows expanding their properties by integrating specific functional groups capable to respond to external stimuli (protons, metal ions, light-irradiation) [12]. Among these, several classes of d⁸-metal complexes where the metal is coordinated to a variety of ligands spanning from nitrogen ligands, cyclometalated, alkynyl to sulfur ligands [13, -21]. An updating on these systems addressed to highlight the special role of related platinum complexes as NLO-active chromophores and their potential for electrooptical devices and optical

communications, can be found in a recent interesting review by V. Guerschais, D. Roberto *et al.* [22]. In D-M-A complexes an asymmetric charge distribution can also be reached where both ligands can be formally taken as dithiolene ligands. As known, dithiolene ligands are capable to undergo reversible redox processes, which involve the filling of the four frontier orbitals (FOs) of π -symmetry (the first two occupied in dithioketone, the third in ene-1,2-dithiolate) as shown in Scheme 1 [23, 24].

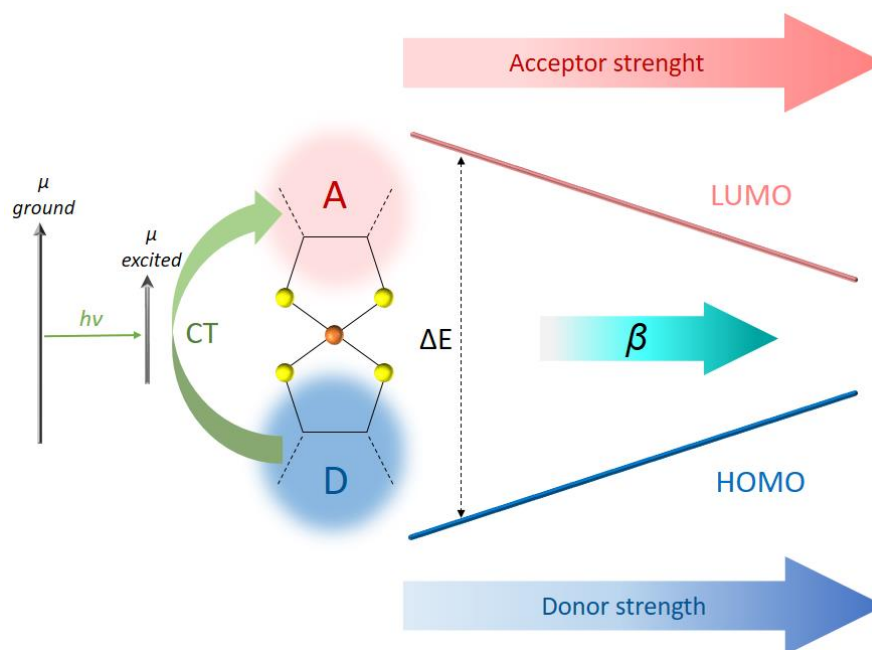


Scheme 1

On the left: redox processes involving α -dithione ligands. On the right: qualitative molecular orbital description

It is well established that the nature of R-substituents affects the energy of these FOs, which are pushed up or down by electron-donating or electron-withdrawing groups respectively, thus stabilizing the dithione or the dithiolate form. Accordingly, the tuning of substituents in heteroleptic dithiolenes where a π -donor (D, the dithiolato) and a π -acceptor (A, the dithione) ligand are connected by a d^8 -metal in a square-planar coordination, allows one to obtain low-energy-gap molecules where the metal acts as a suitable π -bridge for the D-A intramolecular charge transfer (ICT) transition. The ICT Donor–Acceptor process produces a decrease of the dipole moment from the ground to the excited state and, as a consequence, negative solvatochromism and first hyperpolarizability (β) are predictable, in agreement with the two-state theoretical approximation, which takes into account a

single excited state for the dependence of the hyperpolarizability tensor element oriented along the dipolar axis. Accordingly β is directly proportional to $\Delta\mu_{eg}$ (the difference in dipole moment between the lowest unoccupied (LUMO) and the highest occupied (HOMO) molecular orbital), to the square of the transition dipole moment μ_{ge} (oscillator strength) and inversely proportional to the square of ΔE_{ge} , the energy difference between ground and charge transfer excited states [25, 26]. When the electron density is symmetrically distributed along the molecular long axis $\Delta\mu_{eg} \approx 0$ and β will disappear. This approximation provides useful guidelines to synthetic chemists for properly design the components of a D-M-A system. Thus, the CT in these systems controls both the linear and the nonlinear optical properties and can be readily modulated by a proper selection of the ligands, which affect the FOs, as pictorially summarized in Figure 1.



$$\beta \propto \frac{\Delta\mu_{eg}(\mu_{ge})^2}{\Delta E_{ge}^2}$$

Figure 1. Schematic representation of properties tunability in heteroleptic d^8 metal dithiolenes.

In Chart 1 the molecular structures and names of donor and acceptor ligands mentioned in this paper are listed. As far as the Donors are concerned, they differ either for the electron-accepting capability of the substituents at the C2S2 moieties (similar in **D1-D2-D3**; and increasing from **D3** to **D6**) ligand, and/or for the structural features varying from rigid and planar systems (**D1, D5**); to terminal groups connected through a thio-ether bridge (**D2** and **D3**) or conformationally flexible ester groups (**D4**).

The acceptors bear NR groups as electron-donating substituents at the C2S2 moiety. The acyclic dithio-oxamidate (**A1**) [(*R*)- α -MBAdtox] contains the homochiral stereo-center $R=(+)$ α -methylbenzyl and can form a tight ion paired species with HCl (**A1·HCl**), and the cyclic dithioamide R₂pipdt (**A2**) where the NR frames are inserted in a hexa-atomic ring. The accepting capability of these ligands follows the order **A1**<**A1·HCl**<**A2**. The class of dithio-oxamidate ligands and the properties of related metal complexes have been and still are object of an extensive investigation by Campagna, Lanza and co-workers. It has been found that platinum homoleptic complexes coordinated to N,N'-dialkyldithio-oxamidate are capable to work as HCl transporters across a hydrophobic layer over macroscopic distances [27]. Also, the tight-ion paired species formed with HCl by the complex [(HR₂DTO)₂Pt] is capable to donate HCl to an amine. This capability has been successfully exploited for the spectrophotometric determination of aliphatic amines, given that the neutral complex and its HCl tight-ion paired species exhibit different absorptions in the visible region [28]. Moreover, in the solid state, the HCl tight-ion paired species exhibits photoluminescence, which is lost for heating or by exposing the sample to ammonia vapors [29].

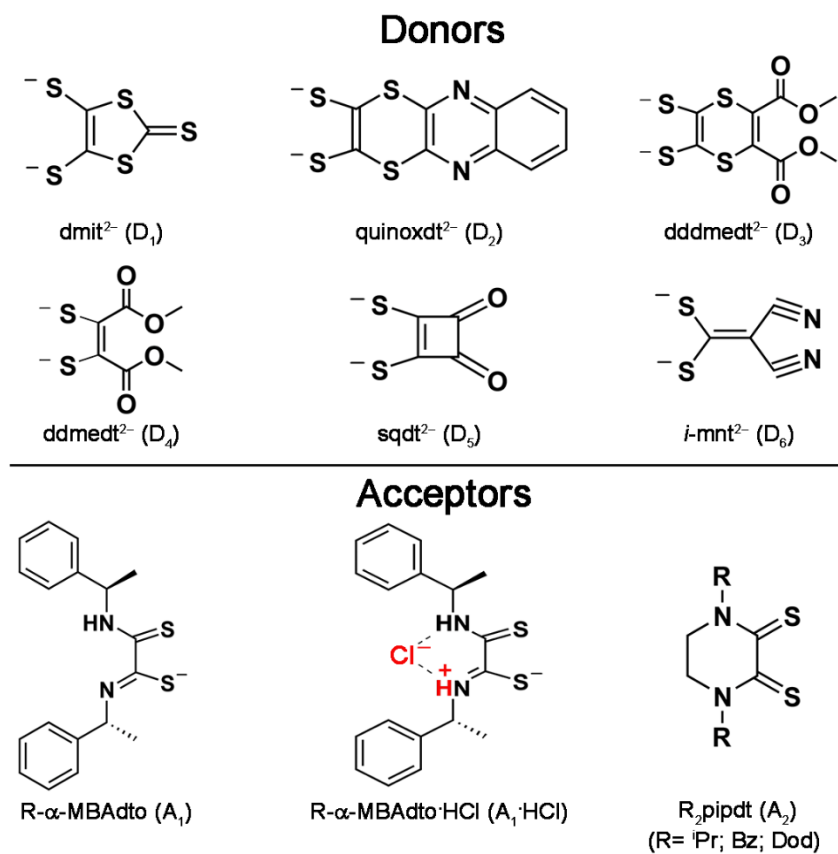


Chart 1

In our previous review published in ICA [27] the role of the ligands and of the metal in affecting the factors which govern the properties as second order NLO chromophores of the following triads [M(Bz₂pipdt)(dmit)]; [M(ⁱPr₂pipdt)(dmit)]; [M(Bn₂pipdt)(dcbdt)] (dcbdt= dicyanobenzodithiolato); [M(Bn₂pipdt)(mnt)] (mnt = maleonitrile-2,3-dithiolate) and [M(Et₂dazdt)(mnt)] (N,N'-diethyl-perhydrodiazepine-2,3-dithione) has been discussed. Structural, electrochemical, spectroscopic, and EFISH measurements as well as DFT and TD-DFT including CPCM methods, have shown that the obtained high negative second-order polarizability values are related to the high difference in dipole moments between excited and ground state enhanced by the electric field of the solvent, the large oscillator strength for the charge transfer transition, and the relatively low energy gap, in agreement with the two-state theoretical approximation (Figure 1). Moreover, steric factors affecting the electronic distribution and thus the NLO properties have been pointed out. It was concluded that the best candidate to maximize the second-order NLO activity among the investigated triads, see Figure

2, results the one composed by Pt(II), R₂pipdt, and dmit, which exhibits the lowest torsion angle between the two thioamido groups of the dithionic ligand and the larger π -system extent of the dithiolato ligand. The reversible bleaching of the solvatochromic peak on monoreduction of these Pd- and Pt-complexes, suggested their potential as switchable redox-active NLO-chromophores.

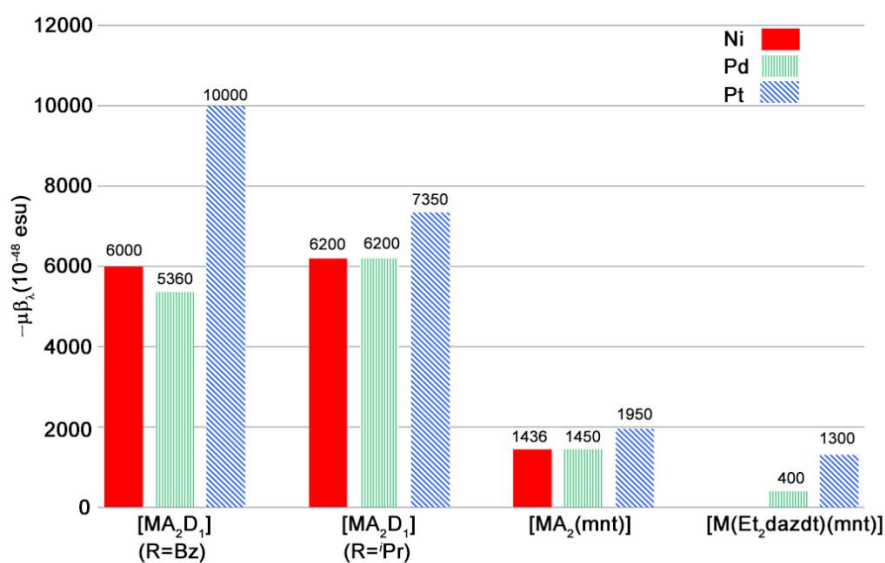


Figure 2. $\mu\beta\lambda$ values of d⁸ metal dithione–dithiolato complexes triads on variation of the metal, the donor and the acceptor ligands.

In this mini-review, the progress of our studies on this class of d⁸metal-heteroleptic complexes, showing the capability of the novel derivatives to respond to external stimuli (protons, silver ions, and light-irradiation) to obtain multifunctional linear and nonlinear chromophores will be presented [31-35]. Promising and less promising results in the production of 2nd NLO-active materials where chromophores are embedded into polymeric PMMA (PolyMethylMethAcrylate) poled films or form crystals belonging to non-centrosymmetric point groups are also here shortly discussed.

Discussion

2. Second-order nonlinear response of d⁸-metal heteroleptic dithiolenes

2.1 Solution 2nd NLO-proton switchable Properties of Complexes sharing the same dithiooxamidate Acceptor (*R*)- α -MBA₂to.

The complexes [MA₁D_n]⁻ shown in Chart 2, have been obtained by combining the Donors **D**₁, **D**₂, and **D**₄ with the Acceptor **A**₁. [32, 36] The Donors, with approximately similar donating properties, are functionalized at the C2S2 moiety with a condensed heterocycle in **D**₁, with a thioether bridge connecting a quinoxaline ring in **D**₂, and two ester groups in **D**₄. The acceptor **A**₁ presents homochiral stereo-centers suitable to promote the crystallization of the compounds in non-centrosymmetric space groups. Moreover, through its capability to undergo proton exchange, NLO switching in these D–M–A systems has been achieved. Structural data of Bu₄N[MA₁D_n] salts helped in elucidating the bonding in these complexes: the metals exhibit a square-planar geometry, with the M–S bond distances derived from the Donor ligand slightly shorter than those derived from the dithiooxamidate ligand. This is in agreement with the different charges of the two ligand systems, 2⁻ for the Donor-dithiolato system and 1⁻ for the Acceptor-dithiooxamidate system. The two SCN moieties of the dithiooxamidate system present bond distances that reflect monoprotection of one N atom with the adjacent C–S fragment with a prevalent thione-nature, while the other C–S fragment exhibits a more pronounced thiolate feature.

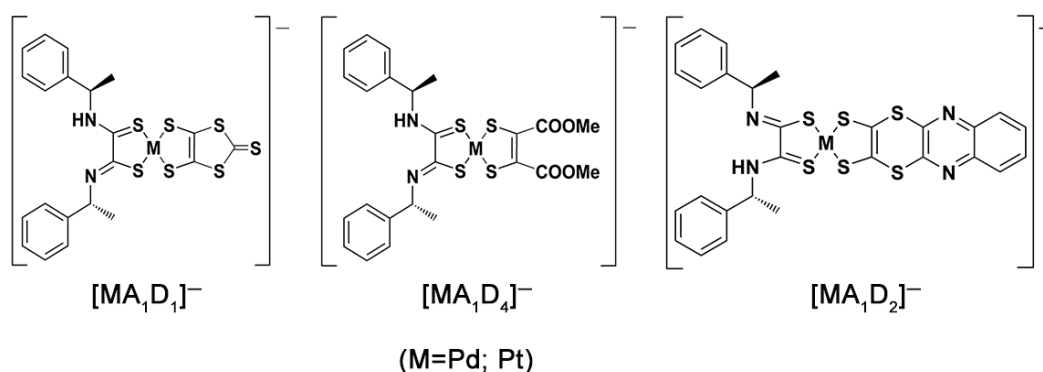


Chart 2

In Table 1 the optical features of the chromophores $[\mathbf{MA}_1\mathbf{D}_n]^-$ ($M = \text{Pd, Pt}; n = 1, 2, 4$) are summarized [36]. On HCl addition the λ_{max} of peaks related to the CT DA transition, undergo a shift to lower frequencies and are recovered for NH_3 addition. On protonation, the negative $\mu\beta_\lambda$ values exhibit a remarkable increase by a factor ranging from 2.5 to 6.5, as a consequence of the increase of the Acceptor character of \mathbf{A}_1 following the formation of the tight-contact ion pair $\mathbf{A}_1\cdot\text{HCl}$ displayed in Figure 3. The process can be reversed, and the $\mu\beta_\lambda$ values of the starting NLO-phores $[\mathbf{MA}_1\mathbf{D}_n]^-$ are fully restored after NH_3 addition as shown for $[\mathbf{PtA}_1\mathbf{D}_4]^-$ in Figure 3 as an example. Thus, on changing the pH, efficient NLO switching is obtained. The $\mu\beta_\lambda$ values of the NLO-chromophores, as well as all those reported in this paper, have been determined by the EFISH (electric-field-induced second-harmonic generation) technique working at non resonant 1907 nm incident wavelength. This technique allows obtaining more reliable data with respect the Hyper-Rayleigh Scattering (HRS) technique, working at 1064 nm and commonly employed to study proton NLO switches in solution, since the possible overestimation of the value of the quadratic hyperpolarizability due to resonance can be prevented.

In addition, the modifications of the linear optical properties, described in the related section, make these complexes valuable multifunctional molecular switches which exhibit contrast in both nonlinear and linear optical properties which can be followed by the naked eyes.

Table 1. Optical properties of $[\text{MA}_1\text{D}_n]^-$ and related tight-ion paired complexes (ref 36)

	$\lambda_{max}(\text{nm})^*$ [$\epsilon \times 10^3$ ($\text{M}^{-1} \text{cm}^{-1}$)]	$\mu\beta_\lambda^{**}$	$\mu\beta_\lambda([\text{MA}_1\text{D}_n]^- \cdot \text{HCl}) / \mu\beta_\lambda([\text{MA}_1\text{D}_n]^-)$		$\lambda_{max}(\text{nm})$ [$\epsilon \times 10^3$ ($\text{M}^{-1} \text{cm}^{-1}$)]	$\mu\beta_\lambda^{**}$	Kurtz	PMMA film (pm V^{-1})
$[\text{PdA}_1\text{D}_1]^-$	525 [15.7]***	-590	3.8	$[\text{PdA}_1\text{D}_1]^- \cdot \text{HCl}$	747 [6.7]	-2210	≈ 0	5.34
$[\text{PtA}_1\text{D}_1]^-$	543 [9.6]***	-1020	2.5	$[\text{PtA}_1\text{D}_1]^- \cdot \text{HCl}$	781 [9.6]	-2560	≈ 0	n. a.
$[\text{PdA}_1\text{D}_4]^-$	525 [4.0]	-390	5.7	$[\text{PdA}_1\text{D}_4]^- \cdot \text{HCl}$	715 [5.7]	-2210	0.2	2.02
$[\text{PtA}_1\text{D}_4]^-$	558 [5.5]	-480	6.5	$[\text{PtA}_1\text{D}_4]^- \cdot \text{HCl}$	764 [11.1]	-3120	0.5	1.32
$[\text{PdA}_1\text{D}_2]^-$	550 [5.5]	-615	3.2	$[\text{PdA}_1\text{D}_2]^- \cdot \text{HCl}$	773 [5.8]	-1970	≈ 0	n. a.
$[\text{PtA}_1\text{D}_2]^-$	606 [6.7]	-735	4.0	$[\text{PtA}_1\text{D}_2]^- \cdot \text{HCl}$	814 [12.4]	-2980	≈ 0	n. a.

*In DMF solutions. ** 10^{-48} esu. ***These values include the contribution from a typical ligand absorption.

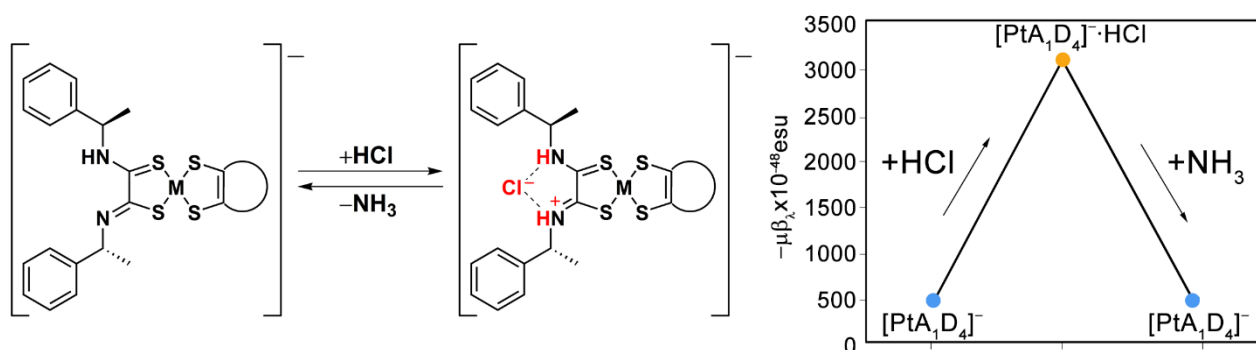


Figure 3. Proton exchange equilibria for $[\text{MA}_1\text{D}_n]^-$ ($n = 1, 2, 4$) and on the right: the NLO proton switch with increase for $[\text{PtA}_1\text{D}_4]^-$ by a factor of 6.5.

2.2. Solution 2nd NLO Properties of Complexes sharing the same Acceptor R₂pipdt.

In Table 2 the optical features of complexes bearing R₂pipdt (**A**₂) as Acceptor are summarized.

Inspection of Table 2 further confirms that inside the D-M-A systems, those based on **M**, **A**₂ and **D**₁ components exhibit the highest values of $\mu\beta_\lambda$, in the Pt-case the highest so far reported for metal complexes, to the best of our knowledge. These values are also higher than those of the corresponding $[\text{MA}_2\text{D}_2]$ compounds, [32] despite both systems exhibit a similar Donor-Acceptor HOMO-LUMO gap, and related absorption maxima. The observed results can be

explained considering the shape of the FOs involved in the CT transitions. In fact, the final states in the **D1** case show a π -orbital system which also involves the periphery of the ligand, differently to the **D2** corresponding orbitals, which are less extended because of the presence of the thio-ether bridges that confer a bended structure to the ligand. On the other side the bended structure of **D2** has shown to be valuable in providing additional peculiar luminescent properties to the derived complexes, as summarized in the related section, making them multi-responsive compounds.

As a last comment on the $\mu\beta_\lambda$ values on corresponding complexes where the central metal is changed (Table 1, Table 2), it can be once more pointed out that platinum derivatives exhibit the highest valued inside the triads. This has been related to the highest metal contribution to the HOMO by the d_{xy} orbital of platinum with respect to that of the other metal centers, so favoring the extent of the π -orbital system and the oscillator strength, as reflected by the observed more intense CT bands [30].

The same **A2** Acceptor (R=Bz) has been employed to synthesize Ni-complexes [**NiA2-D_n**] ($n = 3-6$), on varying the Donor [33]. Despite, as said, the corresponding platinum-complexes would exhibit larger NLO responses, the use of nickel-metal offers advantages in terms of cost and depletion of precious metals and in terms of higher solubility of related complexes in common organic solvents. Thus, it seemed preferable to us to start with nickel complexes to investigate the capability of these class of complexes to be embedded into a poled polymeric matrix to achieve NLO-response in the bulk (see related section). The obtained $\mu\beta_\lambda$ values determined in DMF solution for [**NiA2-D_n**] complexes are still remarkable (Table 2), and their increase is relatable to the λ_{max} increase of the CT absorptions, in agreement with the calculated HOMO-LUMO gap, as shown in Figure 4. Being mainly associated to the acceptor's orbitals, LUMOs energies of these complexes are very similar. Thus, the differences in the FOs gaps between these compounds are mostly related to the energy of the HOMOs.

Table 1. Optical properties of [MA₂D_n]

	$\lambda_{max}(\text{nm})$ * [$\epsilon \times 10^3$ (M ⁻¹ cm ⁻¹)]	$\mu\beta_{\lambda}$ (10 ⁻⁴⁸)esu	PMMA film (pm V ⁻¹)
[NiA ₂ D ₂] ^a <i>R</i> = <i>iPr</i>	863 [8.0]	-1490	n. a.
[PdA ₂ D ₂] ^a <i>R</i> = <i>iPr</i>	773 [3.8]	-1970	n. a.
[PtA ₂ D ₂] ^a <i>R</i> = <i>iPr</i>	836 [10.5]	-4280	n. a.
[NiA ₂ D ₃] ^b <i>R</i> = <i>Bz</i>	678 [6.5]	-680	≈ 0
[NiA ₂ -D ₄] ^b <i>R</i> = <i>Bz</i>	737 [7.4]	-855	≈ 0
[NiA ₂ D ₅] ^b <i>R</i> = <i>Bz</i>	830 [6.1]	-1080	2.20
[NiA ₂ D ₆] ^b <i>R</i> = <i>Bz</i>	872 [8.0]	-1180	≈ 0
[NiA ₂ D ₁] <i>R</i> = <i>Bz</i> ^c	858 [10.6]	-6100	n. a.
<i>R</i> = <i>iPr</i> ^d	827 [8.6]	-6200	n. a.
[PdA ₂ D ₁] <i>R</i> = <i>Bz</i> ^c	819 [11.3]	-5360	n. a.
<i>R</i> = <i>iPr</i> ^d	775 [5.5]	-4700	n. a.
<i>R</i> = <i>Dod</i> ^e	801 [4.4]	-2665	1.86
[PtA ₂ D ₁] <i>R</i> = <i>Bz</i> ^c	827 [14.8]	-10000	n. a.
<i>R</i> = <i>iPr</i> ^d	790 [13.3]	- 7300	n. a.

* In DMF solutions. ^a ref [29]; ^b: ref [30]; ^c ref [36]; ^d ref [37]; ^e ref [38]

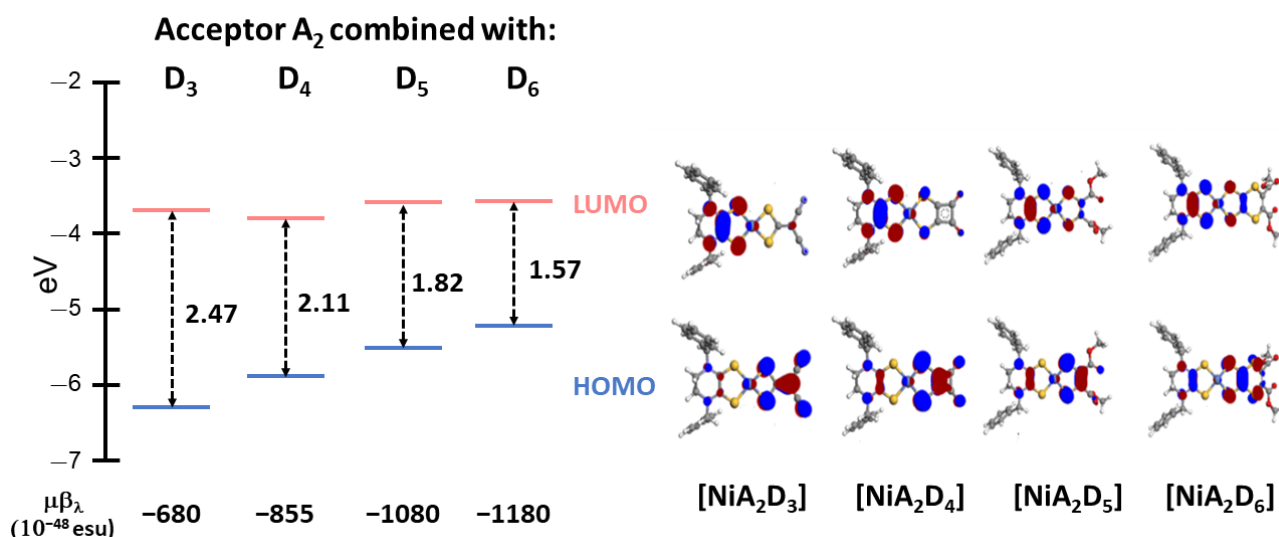


Figure 4. Frontier molecular orbital for [NiA₂D_n]. The Energy gap decrease between the FOs is mainly due to the HOMO's energy level, and is in agreement with the experimentally observed trend in $\mu\beta\lambda$ values

On variation of the Acceptor (Table 1 and Table 2), complexes with the same metal and Donor, show a $\mu\beta\lambda$ increase following the sequence $A_1 < A_1 \cdot HCl < A_2$, according to the increased Acceptor capability. As shown in Figure 5 for D = D₁ the HOMOs energies of these complexes are very similar because they are mainly due to the Donor's orbitals, thus the differences in the FOs gaps between these compounds are mostly related to the energy of the LUMOs.

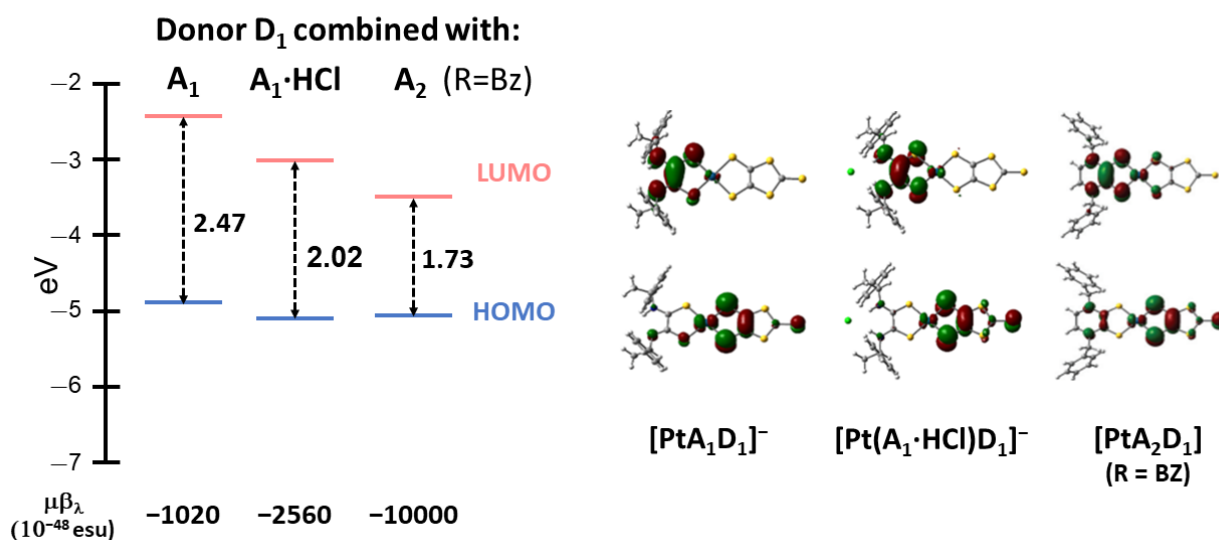


Figure 5. Frontier molecular orbital for [PtA₁D₁]⁻; [Pt(A₁·HCl)D₁]⁻; [PtA₂D₁]⁻. The Energy gap decrease between the FOs is mainly due to the LUMO's energy level.

2.3. 2nd NLO Response in the bulk.

To maintain the 2nd NLO-response in the bulk, the corona-wire poling technique on composite thin films of chromophores dispersed in a polymeric matrix is widely employed [3]. In this technique the starting isotropic material is ordered by the application of a large DC electric field while the material is heated to just below the glass transition temperature (T_g) of the polymeric matrix since the decrease of the viscosity of the matrix near the T_g , allows an easier orientation of the NLO chromophores. After the SHG signal reaches a plateau, the temperature is decreased to room temperature, “freezing” the orientation of the chromophores inside the polymeric matrix, and the electric field is turned off. During the cooling process and after the removal of the electric field, the SHG signal is monitored as a function of time and temperature, to check whether or not reorientation of the chromophores within the polymeric matrix occurs in the explored time and temperature range. This technique has been employed on thin films of **[NiA₂-D_n]** ($A_2 = Bz_2pipdt$, $n = 3-6$) [33] and of **Bu₄N[PdA₁D₁]**; **Bu₄N[PdA₁D₄]** and **Bu₄N[PtA₁D₄]** [35] dispersed in PMMA matrix. The SHG signals, negligible at room temperature, reach a maximum value as the temperature is increased around T_g of the PMMA and the electric field applied. During the cooling process only films of **[NiA₁D₄]** showed a stable SHG response ($\chi_{33}^{(2)} = 2.20 \text{ pm V}^{-1}$), while a fast decrease of the signal of the remaining Ni-based films was observed, despite all the samples exhibited similar thermolytic behaviour. The presence of ester groups attached to the dithiolate moiety in D4 seems to favour a suitable assembly of these NLO-phores in the polymer film to achieve a stable and good SHG response in the bulk. This seems supported by results on thin films of **Bu₄N[PdA₁D₄]** and embedded into PMMA ($\chi_{33}^{(2)} ([PdA_1D_4]) = 2.02 \text{ pm/V}$; $\chi_{33}^{(2)} ([PtA_1D_4]) = 1.32 \text{ pm/V}$) Figure 6. A good and stable response ($\chi_{33}^{(2)} = 5.34 \text{ pm/V}$) was also obtained with **Bu₄N[PdA₁D₁]** bearing dmit as Donor (see Table 1). These good SHG responses seem very promising [22 and related references therein available], however attempts to protonate the films with HCl vapors failed, probably due to the difficulty of the acid to penetrate into

the polymeric PMMA matrix. Replacement of PMMA by different polymer will be pursued to try to obtain the desired goal.

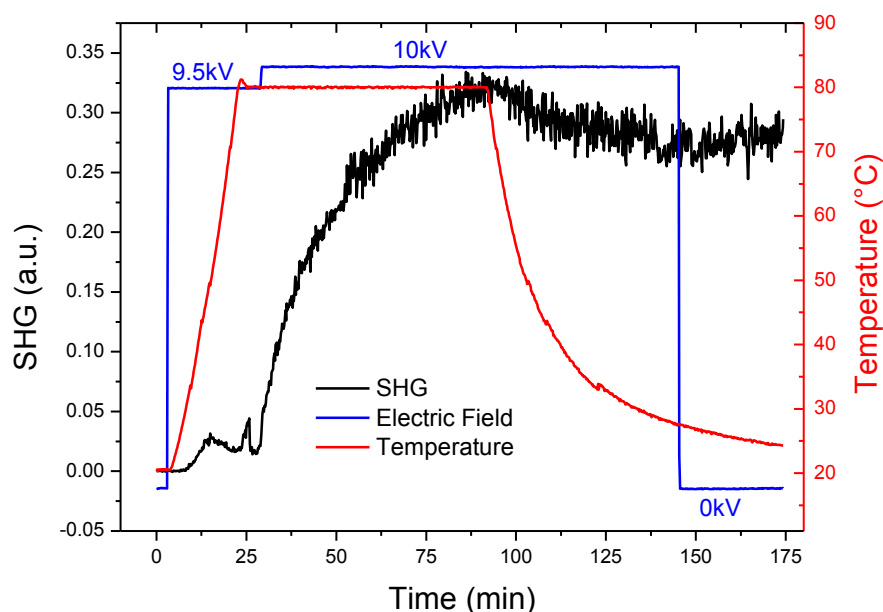


Figure 6. Poling of the **Bu₄N[PtA₁D₄]** PMMA film. SHG (black line) temperature (red line) and electric field (blue line).

The **Bu₄N[MA₁D_n]** (M = Pd, Pt; n = 1, 2, 4) salts, despite crystallizing in non-centrosymmetrical space group, as predictable for the presence of homochiral stereo-centers in (*R*)- α -MBA_{do}, did not show a measurable SHG response, determined according to the Kurtz-Perry method at 1907 nm on crystalline powders, except in the case of **Bu₄N[PtA₁D₄]** (0.5 by comparing intensity with the urea standard). These findings have been ascribed to the different arrangements of the chromophores in the crystals: those containing **D₁** and **D₂** as Donors crystallize in the non-polar *P2₁2₁2₁* space group, which, even though non-centrosymmetric, is one of the unfavorable space groups to allow for a non-null SGH signal. Instead the **Bu₄N[PtA₁D₄]** crystallizes in the polar *P1* space group, and two independent complex molecules, with different orientations, are present in the asymmetric unit, see Figure 7.

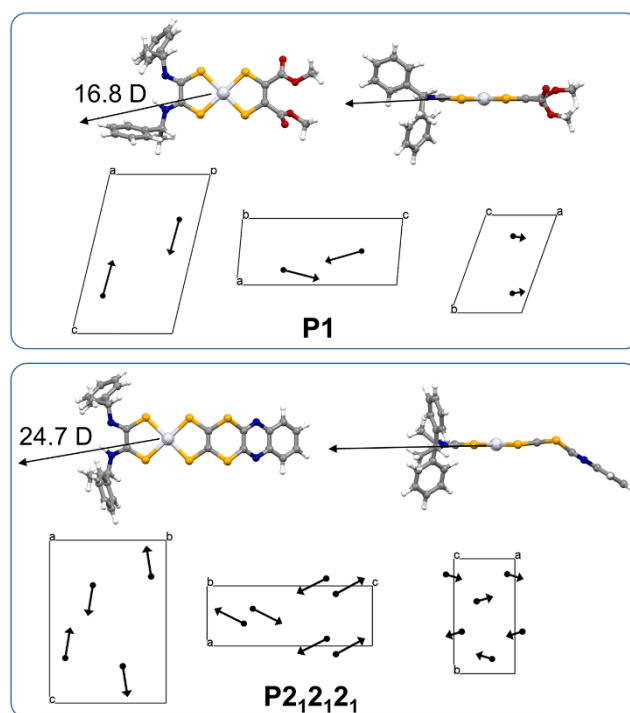


Figure 7. DFT calculated dipole moment and orientation of the dipole moment within the unit cell of $[\text{PtA}_1\text{D}_4]^-$ (above) and $[\text{PtA}_1\text{D}_2]^-$ (below).

In concluding this section it may be underlined that D-M-A complexes based on heteroleptic d^8 -metal dithiolenes well illustrate how all the three components (D-M-A) play a role in affecting the NLO properties of a given complex and further confirm their versatility to control NLO responses by properly engineering the components both to optimize $\mu\beta_\lambda$ values and/or to obtain proton-switching. As far as second harmonic generation in the bulk is concerned, stable and large response was obtained for thin films in few cases. However, failure in protonating PMMA films of the proton switchable NLO-phores, suggests that alternative pathways (different polymeric matrices, or strategies) must be explored to overcome the difficulty of the acid to penetrate the polymeric PMMA matrix. Also, the poor SHG response of crystals clearly shows that further studies-strategies are required to achieve non-centrosymmetric crystals in suitable polar space groups.

3.1 Linear Optical Properties. Proton and Silver Switchable Chromism

Table 1 includes absorptions assigned to the CT Donor–Acceptor transitions of the listed chromophores. The reversible protonation processes for **Bu₄N[MA₁D_n]** (M=Pt, Pd; n=1, 2, 4) described in Section 2.1, is accompanied by a color change in accordance with the shift of the peak to higher wavelengths as shown in Figure 8 for **[PtA₁D₂]⁻** as an example.

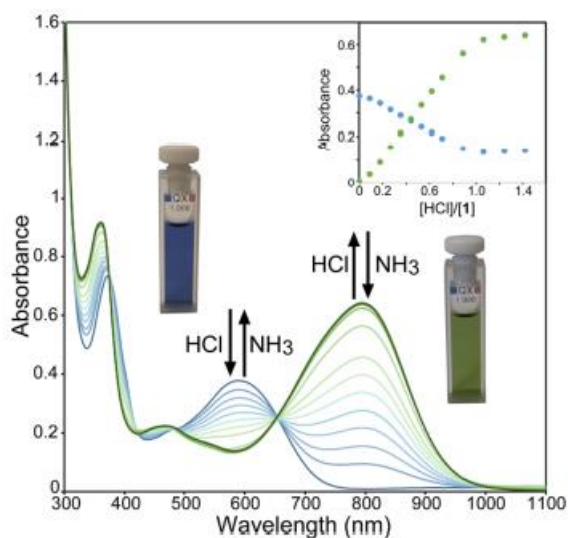


Figure 8. Variation of the absorption upon successive additions of HCl (10 μ L, 10^{-3} M) and NH₃ (10 μ L, 10^{-3} M) to a solution of **[PtA₁D₂]⁻** in CH₃CN (1 mL, 1×10^{-4} M). In the inset, plots of the absorbance values at 588 nm (blue) and 795 nm (green) against [HCl]/[**Bu₄N[PtA₁D₂]⁻]** are reported. Reprinted with permission from ref. [31]. Copyright 2021 American chemical Society.

Interestingly these complexes have shown to be capable to further interact with a different type of electrophile such as the silver ion. In this case the addition of silver trifluoromethanesulfonate (AgOTf) to **Bu₄N[MA₁D_n]** (M=Pt, Pd; n=1, 2, 4) in DMF solutions is accompanied by the formation of a new peak at lower wavelengths. The presence of isosbestic points and the trend of absorbances at λ_{max} versus increasing AgOTf amounts allowed us to reasonably suggest the formation of a 1:2 adduct between the reagents. Removal of silver ions, for example upon HCl addition, allows the recovery of the protonated complexes as shown in Figure 9 for **[PtA₁D₂]⁻** as a representative example.

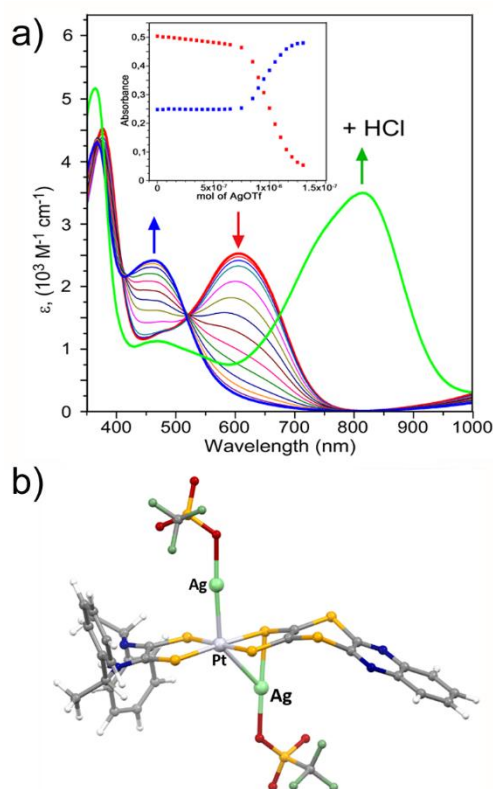


Figure 9. a) UV-vis-NIR spectra of silver titration of $[\text{PtA}_1\text{D}_2]^-$ in DMF solution (concentration 1×10^{-4} M). (b) DFT optimized geometry of $[\text{PtA}_1\text{D}_2] \cdot 2\text{AgOTf}$: B3lyp/6-31+G(d)_SDD with pseudopotentials on Pt (MWB60) and Ag (MWB28) with the PCM method (dimethylformamide). Adapted with permission from ref. [35]. Copyright 2021 American chemical Society.

Computational studies by means of DFT methods and by taking into account the solvent with the polarizable continuum method (PCM) provided great support to elucidate the observed behaviour. In Figure 10 the FOs of $[\text{PtA}_1\text{D}_2]^-$ and of its AgOTf and HCl adducts are displayed as an example. As predictable, the HOMO is mainly localized on the dithiolate system, whereas the LUMO is mainly localized on the dithio-oxamidate fragment. The slightly nonsymmetric shape of the HOMO and LUMO reflects the presence of a hydrogen atom on only one of the thioamido group of the A_1 ligand. A good agreement between the experimental and TD-DFT calculated visible spectra has been found, and it was also confirmed that the low energy absorption band is associated almost exclusively to an HOMO→LUMO transition. The HOMO→LUMO gap increases as a consequence of the HOMO stabilization on formation of the AgOTf adduct, while this gap decreases as a consequence of the LUMO stabilization on

formation of the HCl adduct. In the HCl adduct the most favourable protonation site is the nitrogen atom of A1, with a double N-H...Cl hydrogen bond formation and a consequent more symmetrical shape of the MOs which confers a significant stabilization to the LUMO. This is fully consistent with the observed shift of the low-frequency peak and related color changes.

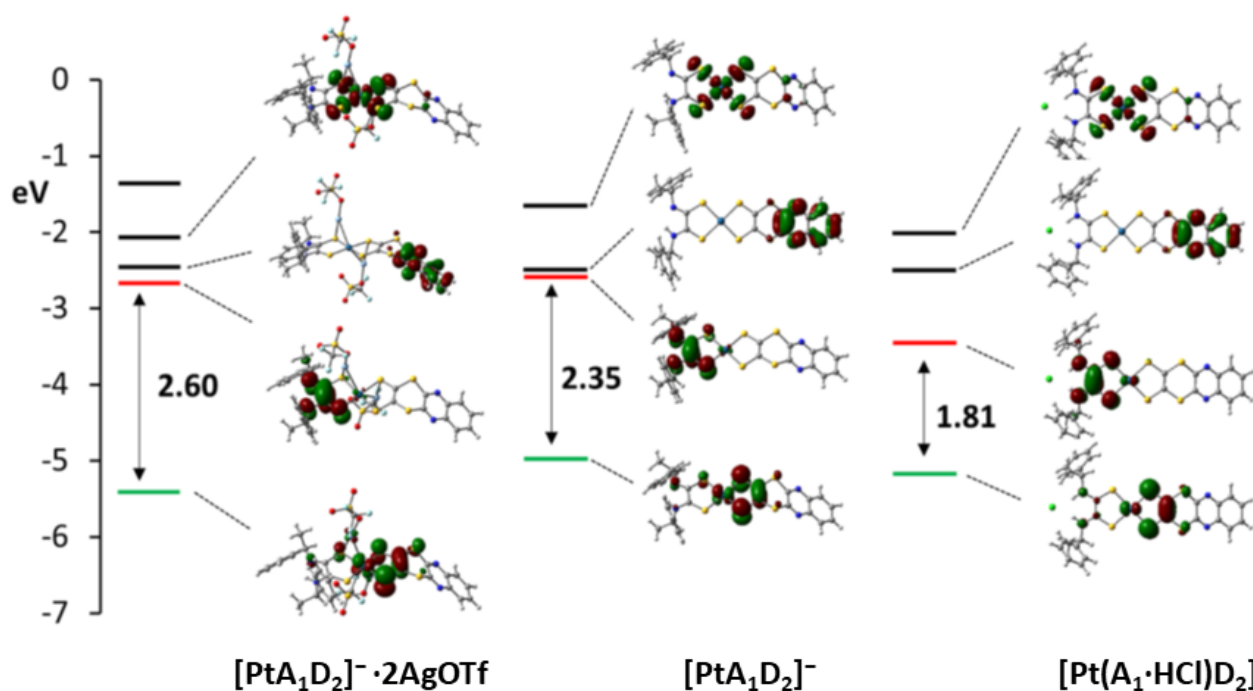


Figure 10. Energy levels and Kohn-Sham MOs for the adducts $[\text{PtA}_1\text{D}_2]^- \cdot 2\text{AgOTf}$ (left), $[\text{PtA}_1\text{D}_2]^-$, and $[\text{Pt}(\text{A}_1 \cdot \text{HCl})\text{D}_2]^-$ (right). The calculations were performed at the B3LYP/6-31+G(d)_SDD level with the PCM method in N,N-dimethylformamide. HOMO green bar, LUMO red bar, energy gap in eV. Reprinted with permission from ref. [35]. Copyright 2021 American chemical Society.

3.2. Linear Optical Properties: Proton and Silver Switchable Photoluminescent Properties

Commonly d^8 metal heteroleptic dithiolene complexes do not exhibit luminescent properties, neither in solution at room temperature nor in glassy solvents at 77 K, with the exception of those containing the quinoxdt donor (D_2). It has been found that both the homoleptic radical $[\text{Pt}(\text{D}_2)_2]^-$ [40] and heteroleptic $[\text{PtA}_1\text{D}_2]^-$ [35] and $[\text{PtA}_2\text{D}_2]$ [32] complexes are emissive in solution at room temperature and, remarkably, the observed emission falls above the energy of the lowest-energy absorption, pointing to an “anti-Kasha”

behaviour [41, 42] (*Kasha's Rule: The emitting level of a given multiplicity is the lowest excited level of that multiplicity*). The origin of this peculiar emissive behaviour is ascribed to the **D₂** ligand and in particular to the sequence and localization of the FOs as calculated from density functional theory (DFT) and schematized in Figure 11a. As it can be seen, the superior excited energy level corresponds to a MO (LUMO+1) that is highly localized on the periphery of the **D₂** ligand. The poor spatial overlap with the LUMO, mainly associated to the dithiolene core, makes the direct (radiative) decay to the ground state (corresponding to the HOMO) kinetically competitive with respect to the commonly observed relaxation through nonradiative interconversion (IC) mechanism between adjacent energy levels. These considerations, together with the significant energy gap between the LUMO+1 and the HOMO -related energy levels justify the observed radiative emission originating from an ILCT transition within the **D₂** ligand of unusual anti-Kasha character. The proposed mechanism has also been validated through advanced transient absorption studies which have allowed tracing back the evolution of the excited states of **[PtA₁D₂]⁻** as representative compound [34]. These studies have highlighted the occurrence of an outstandingly long-lived excited state (1.4 ps in comparison to the typical sub-fs lifetimes of IC) compatible with an emission mechanism stemming from the second excited state.

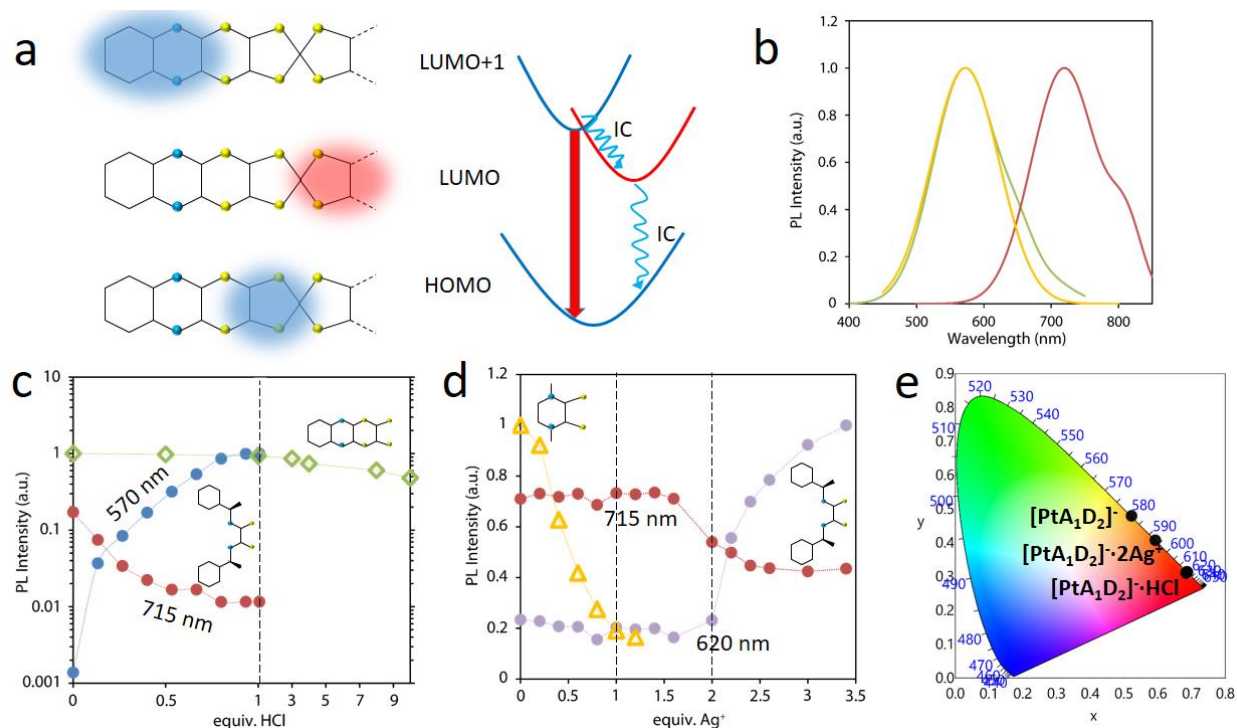


Figure 11. a) General simplified scheme of the frontier MOs and mechanism of anti-Kasha-emission (red arrow) in platinum derivatives with the ligand D_2 ; b) normalized emission spectra of the heteroleptic $[PtA_1D_2]^-$ (red), $[PtA_2D_2]$ (yellow) and of the homoleptic radical $[Pt(D_2)_2]^-$ complexes (green) in DMF solution; c) PL emission intensity plotted on a logarithmic scale as a function of the equivalents of HCl added for $[PtA_1D_2]^-$ (circles) and $[Pt(D_2)_2]^-$ (diamonds).; d) PL emission intensity as a function of the equivalents of Ag^+ added for $[PtA_1D_2]^-$ (circles) and $[PtA_2D_2]$ (triangles). Dashed lines are a guide to the eye. The insets show the structure of the ligands completing the $Pt-D_2$ backbone sketched in a). e) CIE1931 diagram reporting the emission colors of $[PtA_1D_2]^-$, its silver adduct $[[PtA_1D_2]^- \cdot 2Ag^+]$ and its tight-ion paired species with HCl $[[Pt(A_1 \cdot HCl)D_2]^-]$.

Figure 11b shows the steady-state photoluminescence (PL) spectra of the D_2 ligand derivatives in DMF solution upon irradiation in the range 420-450 nm. As anticipated, photoexcitation is solely possible in a spectral region well above the lowest absorption band of the compounds falling in the visible region and typically corresponding to an HOMO-LUMO transition of LL'CT character (see diagram of Figure 11a). Interestingly, while $[Pt(D_2)_2]^-$ and $[PtA_2D_2]$ show a similar emission spectrum peaked at ca. 570 nm and corresponding to a yellow emission, in $[PtA_1D_2]^-$ the LUMO+1 is stabilized resulting in a peculiar emission in the deep red region with a maximum at 715 nm. More importantly, all these systems show reversible stimuli-responsive luminescence responding to acid (HCl) (Figure 11c) and silver triflate addition (Figure 11d). Protonation on the nitrogen donor

atoms of the quinoxaline ring (where the LUMO+1 is mainly located) in $[\text{Pt}(\text{D}_2)_2]^-$ causes a change of the distribution of the electron density resulting in the quenching of the emission. However, initial conditions can be fully restored on addition of ammonia. Similar considerations can be made for the behaviour of $[\text{PtA}_2\text{D}_2]$ upon silver triflate addition (Figure 11d), which quenches the emission as a consequence of the formation of an adduct involving an interaction between the silver ion and the sulphur atoms on the dithiolene core. This adduct formation affects the distribution of the electron density and the sequence of the MOs (in particular the LUMO and LUMO+1, Figure 12) providing an alternative excited state deactivation channel through the $d\sigma^*$ orbitals of Ag^+ . In this case, reversibility of the system properties is obtained after the addition of stoichiometric amounts of HCl which sequesters the Ag^+ ions from the adduct yielding the pristine complex. Contrary to the emission turn off observed in $[\text{Pt}(\text{D}_2)_2]^-$ and $[\text{PtA}_2\text{D}_2]$, $[\text{PtA}_1\text{D}_2]^-$ presents a remarkable luminescence colour switch both in the presence of HCl and silver triflate. As shown in Figure 3, the dithioxamidate ligand **A**₁ can accommodate the HCl molecule yielding a tight-ion paired species of the compound. As highlighted by DFT calculations, this interaction causes a destabilization of the LUMO+1 leading to an increased energy gap with the upper energy levels and justifying the observed blue shift of the emission turning from deep red to yellow-green ($\lambda_{\text{max}} = 570 \text{ nm}$, Figure 11c). Once again, the addition of ammonia fully recovers the pristine compound. Similar considerations can be drawn for the interaction of $[\text{PtA}_1\text{D}_2]^-$ with silver triflate, which, contrary to the above cited case of $[\text{PtA}_2\text{D}_2]$, leaves the MOs sequence unaltered after the formation of a 2:1 adduct, but induces an increment of the energy gap of the ground and emissive levels. This results in an emission colour shifting to orange ($\lambda_{\text{max}} = 620 \text{ nm}$, Figure 11d) which can be reversed to the original deep red on NH_3 or HCl addition. $[\text{PtA}_1\text{D}_2]^-$ represents a quite unique example of a fully reversible “turn on” luminescence sensor which displays emission in three different spectral ranges upon response to diverse stimuli (Figure 11e). This behaviour is realized thanks to

the synergistic effect of the emissive **D₂** ligand and the capability of the chiral **A₁** ligand to interact with external analytes in specific modes. The analogous palladium complex displays similar properties, where the emission colour is modulated by the effect of the different metal ion involved. These results highlight the potential of these compounds for various applications in sensing.

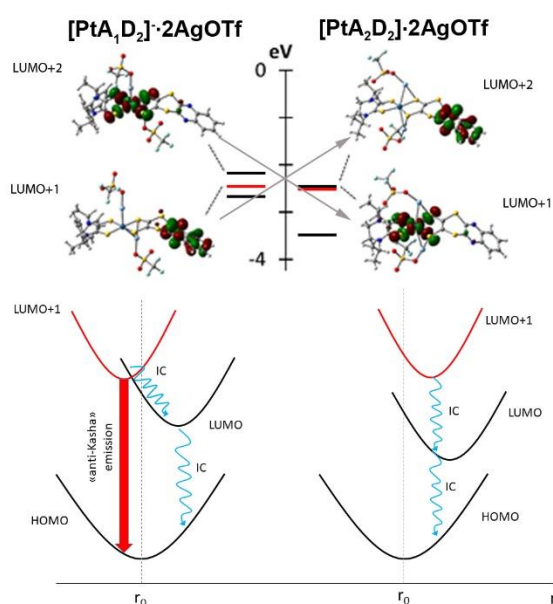


Figure 12. Comparison of the virtual MOs (above) and simplified scheme of the relaxation from the second superior excited state (corresponding to the LUMO+1) of $[\text{PtA}_1\text{D}_2]\cdot 2\text{AgOTf}$ (left) and $[\text{PtA}_2\text{D}_2]\cdot 2\text{AgOTf}$ (right) (below). The LUMO+1 is depicted in blue. r is the molecular coordinate and r_0 is the equilibrium coordinate of the ground state (taken as the HOMO). IC = internal relaxation.

4. Final remarks

This mini-review has been addressed to survey the progress of the studies on heteroleptic d^8 -metal dithiolenes exhibiting linear and non-linear optical properties. The Donors (dithiolato) and Acceptors (dithioxamide and dithioxamidate) of interest in this review, exhibit different electronic and/or structural features, varying from rigid and planar systems to conformationally-flexible ones. The obtained complexes show large quadratic hyperpolarizability, tunable on tuning each of the D–M–A

components. Each of these components contributes in modulating both the energy and topology of the frontier molecular orbitals that are involved in the D-A charge transfer process mediated by the metal. D and A ligands, combined with Platinum and capable to form an extended π -orbital system including metal-d orbitals, confirm to be the most suitable to provide a low HOMO-LUMO gap, an excited-state dipole moment lower from the ground-state one, a large oscillator strength, and consequently high values of the negative quadratic hyperpolarizability. Moreover, on widening the functionality of the D and A components, switchable non-linear and linear chromophores capable to respond to external stimuli (non-linear: proton-responsive; linear: proton and silver-responsive; light-irradiation) have been obtained. Worthy to note, D-M-A (D = **D**₂ = quinoxdt and A= **A**₁= [(R)- α -MBA₂tox]) complexes, in addition to proton switchable NLO-properties, show emissive properties that are unique inside this class of compounds. This is achieved thanks to the combined action of **A**₁, able to react with protons, and **D**₂, carrier of luminescent properties and capable to interact with silver ions. It can be remarked that the properties of these multi-responsive optical switches can be followed by the naked eye. Computational studies have shown to be useful to rationalize the experimental results and provide useful suggestions for future works to finely design the components to reach the desired properties. Attempts to transfer the NLO-properties in the bulk were successful for chromophores dispersed in PMMA films in a limited number of cases. As crystals, complexes bearing **A**₁, despite crystallizing in non-centrosymmetrical space group for the presence of homochiral stereocenters in **A**₁, show a weak or not measurable SHG response. This is relatable to unfavourable orientation of molecules in the asymmetric unit. Reported achievements and failures are addressed to stimulate future work to exploit the potential of this class of complexes as linear and non-linear optical molecular sensors and switches and to optimize the processing procedures to achieve good SHG responses in the bulk.

Aknowledgements

The work of collaborators who have cooperated along the years to this topic are gratefully acknowledged. In particular to achieve the results reviewed here, the contributions of Dr Salahuddin S. Attar for the synthesis and characterization; of Prof. A. Cannizzo for the photoemissive properties; of Prof. M. Pizzotti and collaborators for the NLO-properties were crucial.

References

- [1] R. W. Boyd, *Nonlinear Optics*, ed., Academic Press, New York, 1992, G.S. He (Ed.), *Nonlinear Optics and Photonics*, Oxford University Press, Oxford, 2015.
- [2] P. N. Prasad, D. J. Williams, *Introduction to Nonlinear Optical Effects in Molecules and Polymer*, ed., John Wiley & Sons, New York, 1991.
- [3] L. R. Dalton, P. A. Sullivan, D. H. Bale, *Electric Field Poled Organic Electro-optic Materials: State of the Art and Future Prospects*, *Chem. Rev.* 110 (2010) 25.
- [4] G. G. A. Balavoine, J-C. Daran, G. Iftime, P. G. Lacroix, E. Manoury, J. A. Delaire, I. Maltey-Fanton, K. Nakatani, S. Di Bella, *Organometallics* 18 (1999), 18, 21-29.
- [5] M. Li, Y. Li, H. Zhang, S. Wang, Y. Ao and Z. Cui, *Molecular engineering of organic chromophores and polymers for enhanced bulk second-order optical nonlinearity*, *J. Mater. Chem. C*, 5 (2017) 4111-4122.
- [6] D. R. Kanis, M.A. Ratner, T.J. Marks, *Optical nonlinearities of conjugated molecules. Stilbene derivatives and highly polar aromatic compounds*, *Chem. Rev.* 67 (1994) 195-242.
- [7] J. Wu, B. A. Wilson, D. W. Smith Jr., S. O. Nielsen, *Towards an understanding of structure/nonlinearity relationships in triarylamine-based push-pull electro-optic chromophores: the influence of substituent and molecular conformation on molecular hyperpolarizabilities*, *J. Mater. Chem. C*, 2 (2014) 2591–2599.
- [8] P. Beaujean, F. Bondu, A. Plaquet, J. Garcia-Amoros, J. Cusido, F. M. Raymo, F. Castet, V. Rodriguez, B. Champagne, *Oxazines: A New Class of Second-Order Nonlinear Optical Switches*, *J. Am. Chem. Soc.* 138 (2016) 5052–5062.
- [9] P. S. Marqués, J. M. A. Castàn, B. A. L. Raul, G. Londi, I. Ramirez, M. S. Pshenichnikov, D. Beljonne, K. Walzer, M. Blais, M. Allain, C. Cabanetos, P. Blanchard, *Triphenylamine/Tetracyanobutadiene-Based π -Conjugated Push–Pull Molecules End-Capped with Arene Platforms: Synthesis, Photophysics, and Photovoltaic Response*, *Chem. Eur. J.* 26 (2020) 16422 – 16433.
- [10] T. Yanbe, K. Mizuguchi, R. Yamakado S. Okada, *Optical property control of p-electronic systems bearing Lewis pairs by ion coordination*, *Chem. Commun.* 56 (2020) 10654-10657.
- [11] B.J. Coe, *Comprehensive Coordination Chemistry II*, J.A. McCleverty, T.J. Meyer TJ Eds., Elsevier Pergamon Oxford, U.K., *Nonlinear Optical Properties of Metal Complexes*, 9 (2004) 621-687.
- [12] S. Di Bella, C. Dragonetti, M. Pizzotti, D. Roberto, F. Tessore, R. Ugo, *Topics in Organometallic Chemistry 28. Molecular Organometallic Materials for Optics*, H. Le Bozec, V. and Guerchais (eds.), Springer Verlag Berlin Heidelberg 28 (2010), 1.
- [13] D. Roberto, R. Ugo, F. Tessore, E. Lucenti, S. Quici, S. Vezza, P.C. Fantucci, I. Invernizzi, S. Bruni, I. Ledoux-Rak, J. Zyss, *Effect of the Coordination to M(II) Metal Centers (M = Zn, Cd, Pt) on the Quadratic Hyperpolarizability of Various Substituted 5-X-1,10-phenanthrolines (X = Donor Group) and of trans-4-(Dimethylamino)-4'-stilbazole*, *Organometallics* 21 (2002) 161- 170.

- [14] F. Nisic, E. Cariati, A. Colombo, C. Dragonetti, S. Fantacci, E. Garoni, E. Lucenti, S. Righetto, D. Roberto, J. A. Gareth Williams, 'Tuning the dipolar second-order nonlinear optical properties of 5- π -delocalized-donor-1,3-di(2-pyridyl) benzenes, related cyclometallated platinum(II) complexes and methylated salts, Dalton Trans. 46 (2017) 1179–1185.
- [15] G. D. Batema, M. Lutz, A. L. Spek, C. A. van Walree, G.P.M. van Klink, G. van Koten, Organometallic benzylidene anilines: donor–acceptor features in NCN-pincer Pt(II) complexes with a 4-(E)-[(4-R-phenyl)imino]methyl substituent, Dalton Trans. 43 (2014) 12200-12209.
- [16] R. D'Amato, A. Furlani, M. Colapietro, G. Portalone, M. Casalboni, M. Falconieri, M. V. Russo, Synthesis, characterisation and optical properties of symmetrical and unsymmetrical Pt(II) and Pd(II) bis-acetylides. Crystal structure of trans-[Pt(PPh₃)₂(CC–C₆H₅)(CC–C₆H₄NO₂)], J. Organomet. Chem. 627 (2001) 13–22.
- [17] R. J. Durand, S. Gauthier, S. Achelle, S. Kahlal, J.-Y. Saillard, A. Barsella, L. Wojcik, N. Le Poul, F. Robin-Le Guen, Incorporation of a platinum center in the pi-conjugated core of push–pull chromophores for nonlinear optics (NLO), Dalton Trans. 46 (2017) 3059–3069;
- [18] S. D. Cummings, L.T. Cheng, R. Eisenberg, Metalloorganic Compounds for Nonlinear Optics: Molecular Hyperpolarizabilities of M(diimine)(dithiolate) Complexes (M = Pt, Pd, Ni), Chem. Mater. 9 (1997) 440–450.
- [19] L. Pilia, M. Pizzotti, F. Tessore, N. Robertson, N. Nonlinear-optical properties of α -diiminedithiolato nickel(II) complexes enhanced by electron-withdrawing carboxyl groups, Inorg. Chem. 56 (2014) 4517-4526.
- [20] G. Li, M. F. Mark, H. Lv, D. W. McCamant, R. Eisenberg, Rhodamine-Platinum Diimine Dithiolate Complex Dyads as Efficient and Robust Photosensitizers for Light-Driven Aqueous Proton Reduction to Hydrogen, J. Am. Chem. Soc. 140 (7) (2018) 2575-2586;
- [21] L. Linfoot, P. Richardson, K. L. McCall, J. R. Durrant, A. Morandeira, N. Robertson, A nickel-complex sensitiser for dye-sensitised solar cells. Solar Energy, 85 (2011) 1195-1200.
- [22] A. Colombo, C. Dragonetti, V. Guerchais, D. Roberto, An excursion in the second-order nonlinear optical properties of platinum complexes; Coord. Chem. Rev. 446 (2021) 214113.
- [23] Dithiolene Chemistry: Synthesis, Properties and Applications, Progress in Inorganic Chemistry, Vol.52, Special Vol. Ed. by E. I. Steifel, 2004 John Wiley&Sons, Inc, Hoboken, New Jersey;
- [24] S. Sproules, K. Wieghardt, Dithiolene radicals: Sulfur K-edge X-ray absorption spectroscopy and Harry's intuition. Coord. Chem. Rev. 255 (2011) 837–860.
- [25] J. L. Oudar, D.S. Chemla, Hyperpolarizabilities of the nitroanilines and their relations to the excited state dipole moment, J. Chem. Phys. 66 (1977) 2664-2668.
- [26] J. L. Oudar, Optical nonlinearities of conjugated molecules. Stilbene derivatives and highly polar aromatic compounds, J. Chem. Phys. 67 (1977) 446-457.
- [27] A. Giannetto, S. Lanza, F. Puntoriero, M. Cordaro, S. Campagna, Fast transport of HCl across a hydrophobic layer over macroscopic distances by using a Pt(II) compound as the transporter; Chem. Commun. 49 (2013) 7611-7613.
- [28] A. Giannetto, M. Cordaro, S. Campagna, and S. Lanza, Metal Complexes as Self-Indicating Titrants for Acid–Base Reactions in Chloroform, Inorg. Chem. 57 (2018) 2175-2183.
- [29] F. Nastasi, F. Puntoriero, N. Palmeri, S. Cavallaro, S. Campagna, S. Lanza, Solid-state luminescence switching of platinum(II) dithiooxamide complexes in the presence of hydrogen halide and amine gases, Chem. Commun. (2007) 4740-4742.
- [30] D. Espa, L. Pilia, S. Attar, A. Serpe, P. Deplano, Molecular engineering of heteroleptic metal-dithiolene complexes with optimized second-order NLO response, Inorg. Chimica Acta, 470 (2018) 295-302.

- [31] S. S. Attar, D. Espa, F. Artizzu, L. Pilia, A. Serpe, M. Pizzotti, G. Di Carlo, L. Marchiò, P. Deplano "Optically Multiresponsive Heteroleptic Platinum-dithiolene Complex with Proton Switchable Properties" *Inorganic Chemistry*, 56 (2017) 6763–6767.
- [32] S. S. Attar, F. Artizzu, L. Marchiò, D. Espa, L. Pilia, M. F. Casula, A. Serpe, M. Pizzotti, A. Orbelli Biroli, P. Deplano, Uncommon Optical Properties and Silver-responsive Turn-off/on Luminescence in a Pt(II) heteroleptic dithiolene complex, *Chem. Eur. J.* 24(2018) 10503-10512.
- [33] S. S. Attar, L. Marchiò, L. Pilia, M. F. Casula, D. Espa, A. Serpe, M. Pizzotti, D. Marinotto, P. Deplano; Design of Nickel Donor-Acceptor Dithiolenes for 2nd order Nonlinear Optics. Experimental and Computational study, *New Journal of Chemistry*, 46 (2019) 12570-12579.
- [34] M. Gazzetto, F. Artizzu, S. Attar, L. Marchio', L. Pilia, E. Rohwer, T. Feurer, P. Deplano, A. Cannizzo, "Anti-Kasha Conformational Photo-isomerization of a Heteroleptic Dithiolene Metal Complex Revealed by Ultrafast Spectroscopy" *The Journal of Physical Chemistry, Part A* 124(51) (2020) 10687-10693.
- [35] S. S. Attar, L. Pilia, D. Espa, F. Artizzu, A. Serpe, M. Pizzotti, D. Marinotto, L. Marchiò, P. Deplano, An insight into the properties of heteroleptic metal dithiolenes: Multi-Stimuli Responsive Luminescence, Chromism and Nonlinear optics, *Inorg. Chem.* 60 (13) (2021) 9332-9344.
- [36] D. Espa, L. Pilia, L. Marchio, M. L. Mercuri, A. Serpe, A. Barsella, A. Fort, S. J. Dalglish, N. Robertson, P. Deplano, Redox Switchable Chromophores based on Metal (Ni, Pd, Pt) Mixed-Ligand Dithiolene Complexes Showing Molecular Second-order NLO Activity, *Inorg.Chem.* 50 (2011) 2058-2060.
- [37] D. Espa, L. Pilia, L. Marchiò, S. S. Attar, A. Barsella, A. Fort, M. L. Mercuri, A. Serpe, Paola Deplano, Structural changes in MII dithione/dithiolato complexes (M = Ni, Pd, Pt) on varying the dithione functionalization, *CrystEngComm* 17 (2015) 4161-4171.
- [38] D. Espa, L. Pilia, L. Marchiò, F. Artizzu, G. Di Carlo, D. Marinotto, A. Serpe, F. Tessore, P. Deplano, A nonlinear optical active polymer film based on Pd(II) dithione/dithiolate second-order NLO chromophores, *Dalton Trans.* 45 (2016) 17431-17438.
- [39] D. Espa, L. Pilia, L. Marchiò, F. Artizzu, A. Serpe, M. L. Mercuri, D. Simão, M. Almeida, M. Pizzotti, F. Tessore, P. Deplano; Mixed-ligand Pt(II) dithione-dithiolato complexes: influence of the dicyanobenzodithiolato ligand on the second-order NLO properties, *Dalton Trans.* 41 (2012) 3485–3493.
- [40] S. Attar, D. Espa, F. Artizzu, M. L. Mercuri, A. Serpe, E. Sessini, G. Concas, F. Congiu, L. Marchiò, P. Deplano, A platinum-dithiolene monoanionic salt exhibiting multi-properties, including room-temperature proton-dependent solution luminescence, *Inorganic Chemistry*, 55 (2016) 5118-26.
- [41] L. Shi, C. Yan, Z. Guo, W. Chi, W. Liu, X. Liu, H. Tian, W.-H. Zhu, De novo strategy with engineering anti-Kasha/Kasha fluorophores enables reliable ratiometric quantification of biomolecules, *Nat. Commun.* 11 (2020) 793.
- [42] H. Wang, J. Wang, T. Zhang, X. Zhang, H. Sun, Y. Xiao, T. Yu, W. Huang Breaching Kasha's rule for dual emission: mechanisms, materials and applications, *J. Mater. Chem. C* 9 (2021) 10154-10172.